JOINTS 2025; 3: e1397

Category: Original Article

ARTIFICIAL INTELLIGENCE APPLIED TO Q-ANGLE MEASUREMENT: PRELIMINARY RESULTS ON AN ALGORITHM BASED ON BOUNDING BOX

L. ALBERTI[1,2], D. LOIACONO[3], A. FAVARO[2], A. BONDI[2], L. BERTOLINO[2], T. BONANZINGA[1,2]

• • •

[1]Department of Biomedical Sciences, Humanitas University, Via Rita Levi Montalcini 4, Pieve Emanuele, Milan, Italy
[2]IRCCS Humanitas Research Hospital, Via Manzoni 56, Rozzano, Milan, Italy
[3]Dipartimento di Elettronica, Informazione e Bioingegneria, Politecnico di Milano, Milan, Italy

Corresponding Author
Luca Alberti, MD; e-mail: luca.alberti@humanitas.it

ABSTRACT – *Objective:* The measurement of Q-angle lacks standardization, with the potential risk of failing to detect clinically relevant findings and misjudgments on types of interventions needed in patellofemoral pathologies. The aim of this study was to implement a machine-learning model for the accurate and reliable measurement of Q-angle directly from radiographs.

Materials and Methods: A total of 187 radiographs (of which approximately 50 belonging to pediatric patients) were manually annotated for the anterior superior iliac spine (ASIS), the center of the patella, and the tibial tuberosity and then enhanced by means of different image preprocessing techniques. Eighty-five percent of X-rays were used for training and 15% for testing and validation. Prediction performance was tested using the full-leg radiograph (WLR) and the bounding boxes (BB) models in terms of mean squared error compared to the ground truth (key points and Q-angles determined by the operator).

Results: Overall, mean prediction errors were the smallest for the patella and ASIS and the highest for the tibial tuberosity. The BB model yielded smaller mean errors in the prediction of all points and Q-angle compared to WLR (except for tibial tuberosity, which was comparable) and showed the highest agreement with ground truth, with no bias for Q-angle.

Conclusions: This proof-of-concept study supports the use of an AI-driven automatic algorithm to identify the key points for measuring Q angle directly from the patient's radiographs. Results demonstrate the highest reliability with the bounding box approach and the algorithm's ability to correctly identify key points across a heterogeneous patient population.

KEYWORDS: Statistic Q-angle, AI, Machine-learning, Patella femoral pain, Radiographs.

INTRODUCTION

To date, the static Q-angle (QA) remains among the main parameters used to describe lower body alignment and assess factors contributing to patellofemoral pain (PFP)[1-5].

This work is licensed under a Creative Commons Attribution-NonCommercial-ShareAlike 4.0 International License

In general, it is accepted that Q-values exceeding 20 degrees are more often associated with misalignment of the patellar joint and knee extensor dysfunction. However, there are no exact threshold values to discriminate a pathological condition in symptomatic *vs.* asymptomatic patients[1,2,5-7].

Values reported across the literature[8] are heterogeneous, and there is no standardized measurement procedure. This leads to large intra- and inter-operator variability. Importantly, an inaccurate Q-angle measurement may fail to detect clinically relevant findings and entail the potential for misjudgments about the types of interventions needed[9-13].

Several studies[13,14] have attempted to increase Q-angle reliability by standardizing measurement with either goniometric or imaging assessments, which additionally provide information on possible intra-articular, articular cartilage, soft tissue, and osseous pathology plus an additional measurement of tubercle lateralization[13-15]. Yet, large-scale implementation is slow, given the limited availability and costly access to diagnostic imaging.

It is likely that innovation could be achieved through artificial intelligence. Many studies[16] in the field of orthopedics have demonstrated how machine learning (ML) can be trained to detect very subtle patterns, thanks to its potential to handle data that is incomplete, unbalanced, complex, and/or has numerous variables with complex interactions. In many cases, ML models have even been demonstrated to outperform clinicians in the interpretation of radiographs in areas such as fracture assessment and to be capable of elaborating outcomes in text formats similar to medical reporting[17].

However, the application of machine learning (ML) to Q-angle measurement has remained unexplored. Accordingly, we aimed to develop and test an automatized model that accurately and reproducibly predicts the Q-angle directly from the patient's radiographs. Specifically, the present work provides a proof-of-concept, discussing the feasibility of a model based on ML and employing the latest version of the real-time You Only Look Once (YOLO) image detection system.

MATERIALS AND METHODS

The present study was based on a pool of radiographic images, which was used to train an algorithm for automatic Q-angle measurement, as described below.

Study Sample

The study was based on a dataset of radiographic imaging from patients attending the Department of Orthopaedics of our tertiary referral orthopedic institution in northern Italy.

Radiographs were from a representative pool of patients being referred to surgery for growth pathology or hip and knee arthrosis. The age range was from 3 to 88 years, with a mean of 38 years (±SD 21.40) admitted for conditions including growth anomalies, malalignment, and arthrosis. One-third of the patients were pediatric (referred for growth pathologies), while the remaining two-thirds were over 50 years of age (referred for arthrosis pathology).

The dataset included a total of 187 radiographs. The images were randomly divided (split ratio 85:15) into training images and test images to achieve a reasonable representativeness of the training set. Thus, of the total sample, 159 (85%) were used for training (training X-rays) and 28 (15%) (testing X-rays), of which 11 (40%) were used for validation and 17 (60%) were used for testing.

The inclusion of the radiographs in the study was bound to the patient's written consent for the use of their data for scientific purposes in anonymized form upon admission to the radiological ward. Since the study exclusively involved anonymized radiographs, it did not require approval by the Ethics Committee board.

Data Annotation and Preparation

Radiograph annotation and collection

Full-length radiographs of the lower limbs in a standing bipedal position were performed in accordance with routine clinical practice. Each radiograph had been manually annotated by the orthopedic surgeon for the reference points used for Q-angle measurement, i.e., the anterior superior iliac spine (ASIS), the center of the patella and the middle third of the tibial tuberosity (TT). The ASIS was

identified as the superoanterior margin of the iliac crest, visible on X-ray as the protuberance where the iliac crest terminates anteriorly. The TT was identified as the middle third of the proximal tibial metaphysis. The center of the patella was identified as the center of the X-ray of the patella. Such points were then uploaded to a software (OsiriX platform by DICOM Viewer)[18] commonly used in the standard clinical setting for the Q-angle calculation.

All radiographs underwent initial quality control screening for the contrast of radiological imaging and visibility of landmarks of interest (ASIS, center of the patella, and anterior tibial tuberosity). Those with low-quality or unreadable scans (radiological artifacts, presence of fixation devices) that prevented the visualization of the key radiological landmarks were discarded.

The original manual annotations performed on the radiographs served as ground truth for training the model and evaluating its outcome.

Image preprocessing

In order to increase model performance, we tested three different image preprocessing techniques. Specifically:

- Contrast Limited Adaptive Histogram Equalization (CLAHE), which improves the contrast of images by limiting contrast amplification in homogeneous areas, which is particularly effective for medical images[19,20];
- Noise reduction by means of advanced denoising techniques suitable for medical images, i.e., non-local means denoising, which preserves fine details while reducing noise;
- Edge detection, used to enhance the visibility of anatomical structures – crucial for accurately identifying key points in radiographs.

Model Design

Framework

The research question was approached through a machine learning algorithm (ML) as a coordinate regression problem (see **Supplementary File 1**). The objective was to predict the coordinates of key points from the radiographic images, allowing subsequent calculation of the Q-angle.

Given the limited number of available images and the similarity of this task to pose detection, we selected the You Only Look Once, version 8 (YOLOv8) object detection and image segmentation model as a basis for our work. YOLOv8 is a deep learning model optimized for real-time object detection and key point prediction[21-23]. The model divides the input image into a grid and predicts bounding boxes along with associated class probabilities for each grid cell. For pose estimation, it predicts the coordinates of key points within these bounding boxes. In particular, the YOLOv8 pose is specifically designed for joint detection and 2D multi-person pose estimation without the use of heatmaps. This approach allows end-to-end training and optimization of the object key-point similarity metric, directly aligning the training objective with the evaluation metric.

Training

The YOLOv8 model was initially trained on a large-scale object detection dataset, the Common Objects in Context (COCO) dataset, and used to initialize the model for the specific study[24,25]. The model was then fine-tuned on the annotated dataset to adapt it to the specific targets and images involved in Q-angle measurement. All models were trained for a maximum of 500 epochs. Based on the validation set error, early stopping with patience of 100 epochs was used.

Data augmentation

The dataset used to train the models was extended using data augmentation techniques to increase its size and representativeness. Specifically, we applied a series of transformations to the original images (flipping, rotating, scaling, cropping, and changing the brightness and contrast) to expose the

model to a broader spectrum of potential real-life scenarios. This helped the model enhance generalization performance when shifting from the training data to unseen data, reduce overfitting, and improve robustness and performance.

During image transformation, all artifacts or distortions that could mislead the model during the image transformations and hinder its learning process were minimized.

The transformations carried out were as follows: random horizontal flipping (i.e., flipping the images horizontally with a probability of 0.5), mosaic augmentation (i.e., combining four images into one to allow learning in context from different parts of the images), and color augmentations (i.e., adjusting brightness, contrast, and saturation to make the model invariant to different acquisition conditions).

Creation of the model

A first model was developed to process the Whole-Leg Radiograph (WLR), analyzing the entire pelvis and both knees simultaneously. The model's output was an approximate identification of three key points of interest (ASIS, center patella, and tibial tuberosity) for both limbs (Figure 1).

The next step involved generating three bounding boxes (BB) for each of the X-rays, each 800x800 pixels in size, centered on the approximate positions originally predicted by the first model on WLR. These boxes were used to train three specialized prediction models: one for the ASIS, one for the patella, and one for the tibial tuberosity. The three models were then used to fine-tune the prediction of the relevant key points on the X-ray. These points were finally used to calculate the Q-angle for both limbs.

Model evaluation metrics

Model performance was evaluated on the test set using the mean error, which assessed the accuracy of key-point predictions and the Q-angle compared to the ground-truth measurements. Mean absolute error was measured in linear difference (mm), which expresses deviation in space (i.e., medial, lateral, distal).

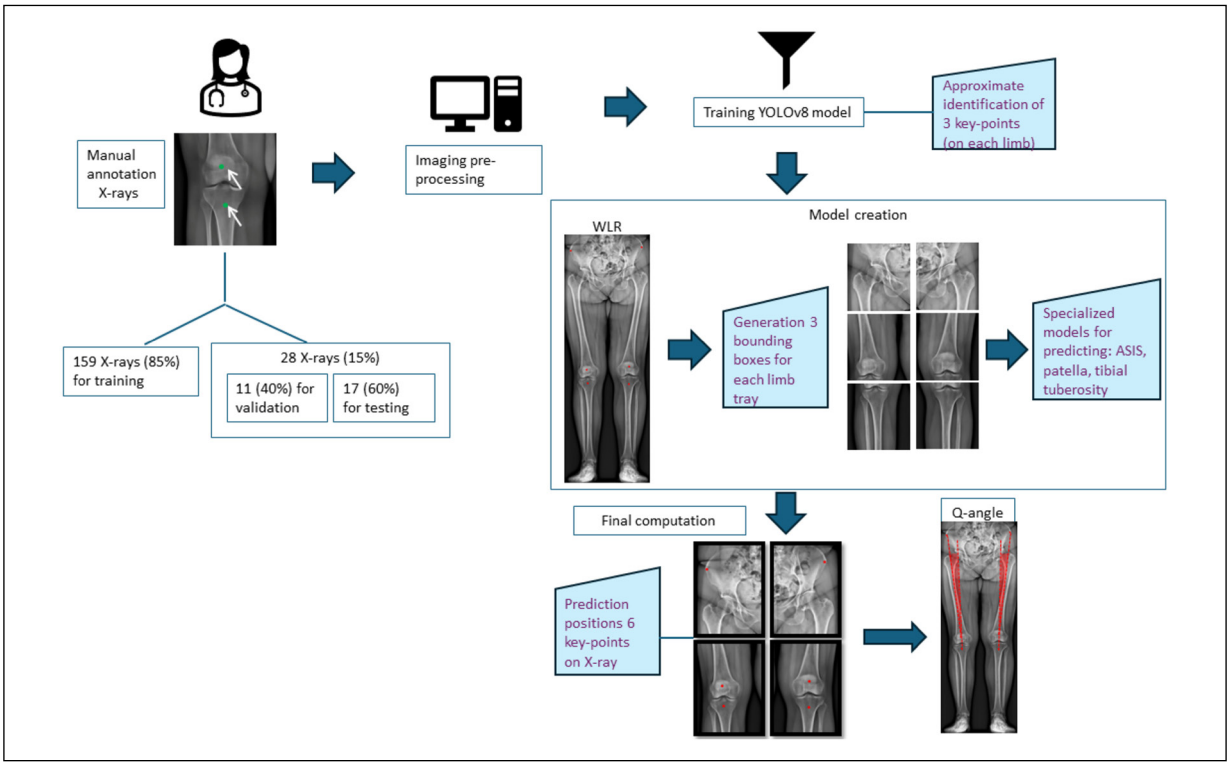

Figure 1. Steps leading to the development of the AI-based model.

Table 1. Mean errors from whole leg radiograph and bounding box models.

Key point	Side	WLR		BB	
		Mean error [mm]	SD	Mean error [mm]	SD
ASIS	R	9.7	4.2	5.9	4.7
	L	8.6	6.3	6.0	4.1
Center of patella	R	6.6	4.1	4.3	2.8
	L	8.5	4.8	4.0	2.0
Tibial tuberosity	R	11.5	5.6	10.3	7.6
	L	11.8	6.9	8.5	5.7

ASIS: Anterior Superior Iliac Spine; BB: bounding box; L: left; SD: standard deviation; R: right; WLR: whole leg radiograph.

RESULTS

The algorithm identified all reference points (axis, patella, and tibial tuberosity) using both the WLR and the BB methods. The position of the reference points obtained by the operator (ground truth) and by the algorithm were compared in terms of distance mean error on prediction and standard deviation (SD). In general, the BB method yielded lower mean errors for all measurement points compared to the WLR, except for the left patella, which featured similar mean errors from both WLR and BB.

As for the values obtained with BB, the shortest distances between operator and algorithm-identified points were observed for the patella, being 4.3 (SD±2.8) and 4.0 (SD±2.0) on the right and left knee, respectively. In contrast, the greatest distance was for tibial tuberosity, with mean errors being 10.3 (SD±7.6) and 8.5 (SD±5.7) on the right and left knee, respectively.

The prediction of mean errors (±SD) observed for WLR and BB models compared to the ground truth are reported in Table 1.

As Q-angle measurements based on operator and algorithm-identified reference points, those measured by BB presented the smallest mean absolute error (MAE) for both legs. Table 2 reports the mean absolute errors (±SD) of the Q-angle as compared to ground truth data.

The degree of agreement for Q-angle values based on the key points measured by WLR and BB against ground truth was assessed by Bland-Altman plots. The WLR approach had a 95% CI ranging from -10 to 16, with a bias of approximately +3 degrees (Figure 2), whereas the BB approach had a 95% CI ranging from -8 to +8, without bias (Figure 3). The higher agreement with BB indicates greater reliability for Q-angle measurement.

Finally, the validation step identified the cases yielding the best and worst agreement of the predicted key points compared to ground truth. Figure 4 is a selection of representative cases.

Table 2. Q-angles measured for the right and left leg separately and for both legs.

Q-angle	Side	WLR		BB	
		Mean absolute error [mm]	SD [mm]	Mean absolute error [mm]	SD [mm]
Q-angle	R	4.7	5.1	2.6	2.6
Q-angle	L	5.5	4.8	3.6	2.9
Q-angle	Both	5.1	5.0	3.1	2.8

BB: bounding box; L: left; SD: standard deviation; R: right; WLR: whole leg radiograph.

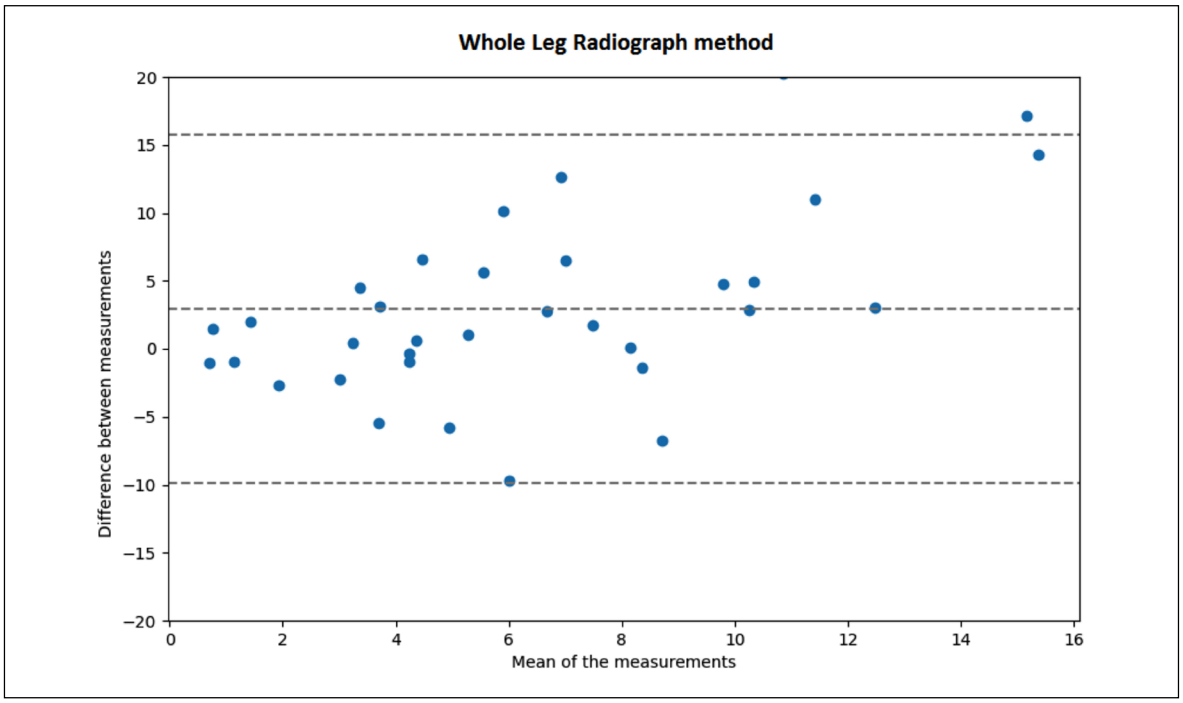

Figure 2. Bland-Altman plot for the whole leg radiograph approach for the approximate key points.

DISCUSSION

The present study proposes a proof of concept for creating an automated model to measure the Q-angle directly from the patient's radiographs. According to the authors' knowledge, this study is the first to report an AI application for the presented objective and highlights its feasibility and strengths, as well as the critical aspects to be addressed in future developments.

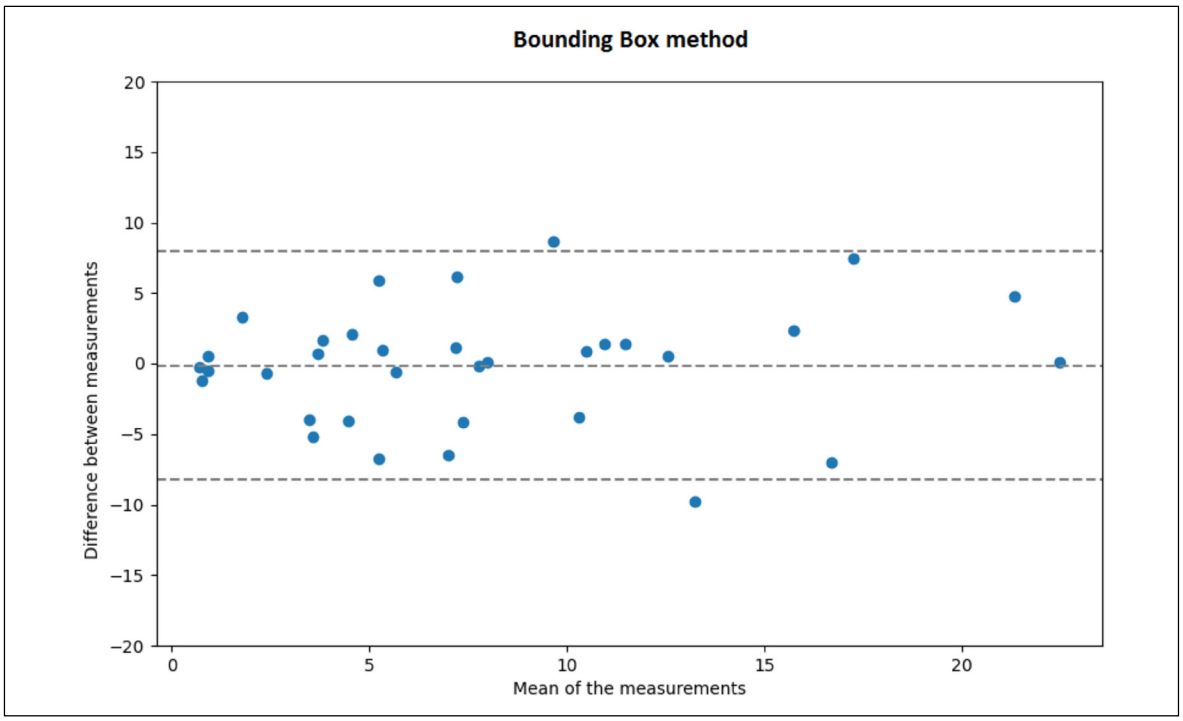

Figure 3. Bland-Altman plot for the bounding box approach for the fine-tuned key points.

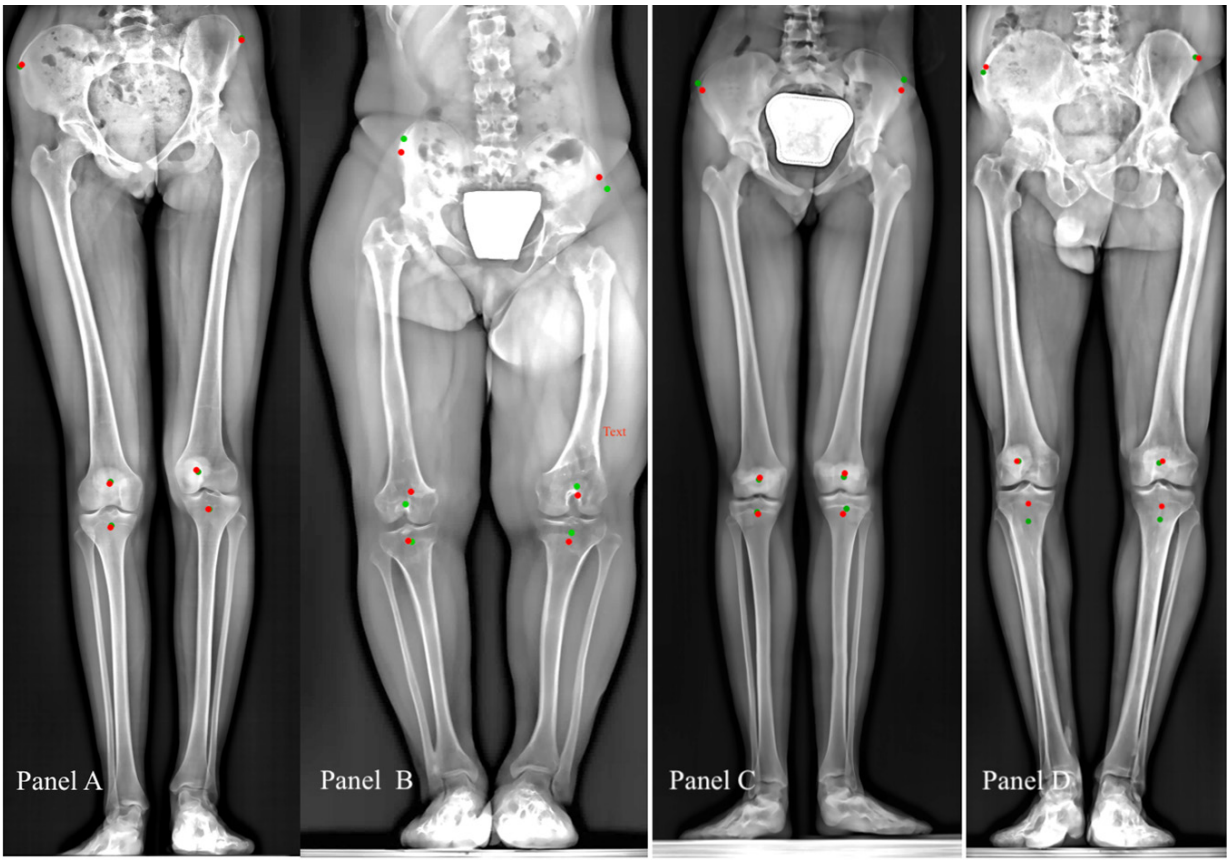

Figure 4. Samples of best and worst agreement compared to ground truth and the predicted key points. Red dots show the prediction by algorithm, green dots: ground truth. **A**, The sample featuring the best agreement. **B-D**, samples yielding the highest discrepancy between manual and predicted key points are reported. Specifically, (**B**) a patient featuring bone structure suggestive of dwarfism; (**C**) tall patient with femoral length at the upper limits; (**D**), a patient standing in tilting position. Here, contrast of images was enhanced to make points more visible.

The idea was developed considering the widespread use of 2D radiographic imaging, which is the most used in current clinical practice due to its relatively low costs compared to those of more sophisticated and less accessible 3D imaging diagnostics.

The model was built with the support of machine learning trained on a dataset of radiographic imaging with manual annotations by an orthopedic surgeon for the ASIS, the center of the patella, and the middle third of the TT. With such data as ground truth, we employed a highly performant real-time object detection and image segmentation model, YOLOv8, and assessed two approaches, the WLR and BB.

Overall, the AI prediction of key points and Q-angle values were coherent with the ground truth and were qualitatively satisfactory for the aim set for the proof-of-concept.

Regarding the Q-angle assessment, BB gave the highest agreement with ground truth with no bias, thus proving its higher reliability. Regarding predicted reference points, BB produced smaller mean distance errors compared to the WLR approach, except for the tibial tuberosity, which resulted in errors comparable to those of both approaches. The mean error for ASIS and patella was less than 5 mm. The mean errors in identification of the reference point for the left leg ranged from 4.3 mm (±2.8) to 10.3 mm (±7.3), with a corresponding mean absolute error for the Q-angle being 2.6 mm (±2.6). Thus, the errors were tolerable and not associated with relevant errors in Q-angle.

These results are also in line with previous studies in the literature addressing Q-angle methodology and accuracy of measurements. One study worth mentioning is that by France and Nester[26], which assessed the effect of error on Q-angle linear measurements. Their results showed that the same range of errors may have different effects in terms of Q-angle based on where these errors are located. Errors between 1 and 5 mm in the medial/lateral location of the center of the patella produced changes in the Q-angle between 1.13 degrees and 5.53 degrees. Errors between 1 and 5

mm in the medial/lateral location of the tibial tuberosity produced changes in the quadriceps angle between 1.02 and 5.18 degrees[26]. In our study, the mean errors for BB were about 4 mm for the center of the patella and about 6 mm for the ASIS and were not associated with any relevant errors in the Q-angle.

Q-Angle Measurement Values and Standard Errors with Traditional Measurements

The potential gain in accuracy by introducing AI to Q-angle measurement may perhaps be appreciated by reviewing previous literature of studies that aimed to improve the reliability of Q-angle measurement by traditional techniques. Weiss et al[9] proposed a repeated-measures design, intratester reliability study using a goniometric assessment on healthy adults. They concluded that the measure was reliable only with patient groups featuring specific characteristics, such as younger age and leaner body composition. Specifically, intraclass correlation coefficient (ICC) (SEM) values were for all subjects 0.88 (1.0°), men 0.77 (1.0°), and women 0.85 (1.0°). Moreover, relevant differences in Q-angles were found only with a 3° difference[9].

Chevidikunnana et al[27] compared QA measurement based on goniometer and radiographic annotation to understand whether these methods featured comparable accuracy and could be used interchangeably[27]. For goniometer-based QA measurement, the assessment was made on the patient's dominant side. For X-rays, patients were positioned supine while maintaining full extension of their knees, with the position fastened with the aid of a wooden block stabilizer. While the authors[27] found a significant relationship between Q-angles obtained using both a goniometer and X-ray imaging ($r=0.91$, $p=0.001$), the difference between the goniometer and X-ray assessment was non-significant, only 0.1°.

In earlier studies, Roush et al[28] challenged the accuracy of goniometer-based assessment against a gold standard computer-based assessment (IMAGEJ by US NIH) to reduce the SEM. Indeed, they observed that the SEM for standard Q-angle measurements reported across literature was 2.4°, which equates to an increase or decrease of the lateral force by 2.9 kilograms for an individual whose quadriceps are generating more than 68 kilograms of force. To achieve greater accuracy, they compared the goniometer-based measurement error for Q-angle (patients in standing position) with computer-based assessment[28]. The ICC was 0.95 (SEM 1.05°) for goniometer-assessed QA and 0.89 (SEM 2.06°) for the computer-based method.

Finally, Merchant et al[13] suggested improving measurement by eliminating patient-related factors (positioning and quadriceps contraction or relaxation) from their goniometric measurement, which contribute to the Q-angle variability they had observed across operators and studies[13]. Measurements were made on a pool of patients without a history of knee problems or a family history of dislocating kneecaps. The mean static Q-angle was 14.8° (≈15°), 95% CI: ±5.4°; the male mean was 13.5°, 95% CI: ±5.2° and the female mean was 15.9°, 95% CI: ±4.8°. No significant difference was found between the right and left knees of males ($p=0.52$), nor of females ($p=0.62$), Beta=0.14. The 2.4° difference between male and female was due to the average height difference between men and women[13].

Factors Affecting the Identification of Reference Points

The closer assessment of mean errors in our study points to several factors that contribute to the predictive accuracy of the reference points. These include both clinical factors (such as pediatric patients featuring open tibial and femoral growth cartilages and subluxated patella of the knee, patients with fixation devices) as well as procedure-related ones (patient positioning during radiographic examination).

In reference to the clinical factors, the heterogeneity of our sample, which included X-rays from patients with a variety of clinical characteristics, is noteworthy. In our study, radiographs from pediatric patients (age range 3-14 years) accounted for 52 of the total 187 in the sample. The inclusion of X-rays from this age group allowed us to have a representative sample for the patient population undergoing knee joint function assessments in our hospital. Moreover, it allowed a heterogeneous dataset for training and testing, which increased the algorithms' robustness, obtaining a model that can be used across multiple clinical practice scenarios. Indeed, it is acknowledged that in patients under the age of 14, the increase in Q-angle above the upper value correlates with a misalignment of the knee extensor apparatus in pediatric patients with knee ligament hyperlaxity and patellar in-

stability[29]. Generally, this feature appears to be associated with a higher rate of lower-limb injuries in young athletes with a risk factor for anterior cruciate ligament (ACL) injury in young female athletes[30,31]. However, values observed in pediatric patients tend to eventually return to typical values with growth. Frequently, extreme values are indices of pathologies such as chondromalacia and patellar luxation that affect the pediatric population[32]. Hence, including radiographs from this patient group will allow us to validate the algorithm in this class of patients as well.

Along the same line, the inclusion of radiographs from adult patients with specific orthopedic conditions allowed us to train the models and strengthen their predictive accuracy. This aspect could also be of future interest in terms of the early detection of signs that require the attention of orthopedics.

Strengths and Limitations

While including a heterogeneous population represents a strength in our methodological approach, we are aware of some limitations affecting the study. Indeed, one is the relatively small sample of radiographs, which will need to be expanded as the algorithm undergoes further fine-tuning. Similar studies generally involve a larger sample, up to ten thousand radiographs. However, given this is a proof of concept, this was not deemed necessary.

Other limitations of the study may be procedure-related biases, both operator-dependant and patient-dependant ones. With specific reference to operator-dependant biases, we may hypothesize this has been a weighing factor in the higher mean errors obtained for the tibial tuberosity with both WLR and BB models. This may be linked to the lack of a distinguishing anatomical feature that prevents the operator from univocally identifying this spot. Indeed, this is acknowledged as a common source of error[26]. Perhaps this could be overcome through the arbitrary identification of a tibial height from which, moving into the central third of the tibial metaphysis, the operator could define an almost standard TT.

On the other hand, accuracy could also be addressed through multiple measurements. The lack of measurements by different operators or by the same operator at different time points in our study prevented us from defining inter- and intra-rater reliability. Measurement by several operators would indeed allow for greater sensitivity and specificity (for example, having measurements by three independent operators).

Finally, one last limitation and area of future research lies in the reduced hyperparameter tuning campaign conducted for the WLR and BB models. A more extensive optimization of the hyperparameters could potentially lead to improved and more robust results, enhancing the performance and reliability of the models.

CONCLUSIONS

This proof-of-concept study supports the use of an AI-driven automatic algorithm in the identification of the key points for Q-angle measurement directly from the patient's radiographs. Results demonstrate the highest reliability with the bounding box approach and the ability of the algorithm to correctly identify key points across a heterogeneous patient population.

Acknowledgments:

The authors are grateful to Manuella Walker for her support in assembling the paper.

Conflict of Interest:

The authors declare they have no conflict of interest in relation to the work herein.

Informed Consent:

Written consent for anonymized data use for scientific purposes was obtained from all patients.

Ethics Approval:

Since the study solely involved radiographic analyses without clinical data and all imaging data were anonymized, no approval from an Ethical Committee board was sought. No supplementary radiographic projections were acquired.

ORCID ID:
Luca Alberti: 0009-0006-1799-8884

Authors' Contributions:
TB, LA, and LD contributed to the development of the idea. LA collected and screened the radiographs, LD performed ML, data acquisition analyses. FA coordinated research methods and result analysis and interpretation; LB contributed to the literature search; TB followed overall supervision of the paper. All authors contributed equally to the development, editing and final approval of the paper.

Funding:
The following project was funded under project No. RCR-2022-23682299 (Title: Medicina in-silico nella diagnosi, prognosi e trattamento dei disordini muscolo scheletrici).

Availability of Data and Materials:
The dataset used for the ML is available upon request to authors and within the purposes of this study.

AI disclosure:
No generative AI was used in the manuscript's writing.

REFERENCES

1. Caylor D, Fites R, Worrell T. The Relationship between Quadriceps Angle and Anterior Knee Pain syndrome. JOSPT 1993; 17: 11-16.
2. Smith T, Nathan A, Hunt J, Donell S. The reliability and validity of the Q-angle: a systematic review. Knee Surg Sports Traumatol Arthrosc 2008; 16: 1068-1079.
3. Almeida GP, Silva AP, França FJ, Magalhães MO, Burke TN, Marques AP. Q-angle in patellofemoral pain: relationship with dynamic knee valgus, hip abductor torque, pain and function. Rev Bras Ortop 2016; 51: 181-186.
4. Kasitinon D, Li WX, Wang EXS, Fredericson M. Physical Examination and Patellofemoral Pain Syndrome: an Updated Review. Curr Rev Musculoskelet Med 2021; 14: 406-412.
5. Milovanović D, Begović N, Bukva B, Dučić S, Vlahović A, Paunović Z, Kadija M, Topalović N, Stijak L. The Influence of the Q-Angle and Muscle Strength on Idiopathic Anterior Knee Pain in Adolescents. Medicina 2023; 59: 1016.
6. Mizuno Y, Kumagai M, Mattessich SM, Elias JJ, Ramrattan N, Cosgarea AJ, Chao EY. Q-angle influences tibiofemoral and patellofemoral kinematics. J Orthop Res 2001; 19: 834-840.
7. Khasawneh RR, Allouh MZ, Abu-El-Rub E. Measurement of the quadriceps (Q) angle with respect to various body parameters in young Arab population. PLoS One 2019; 14: e0218387.
8. Post WR. Clinical evaluation of patients with patellofemoral disorders. Arthroscopy 1999; 15: 841-851.
9. Weiss. L, DeForest B, Hammond K, Schilling B, Ferrira L. Reliability of Goniometry-Based Q-Angle. PM R 2013; 5: 763-768.
10. Olerud C, Berg P. The variation of Q angle with different positions of the foot. Clin Orthop Relat Res 1984; 191: 162-165.
11. Tomsich DA, Nitz AJ, Threlkeld AJ, Shapiro R. Patellofemoral alignment: reliability. J Orthop Sports Phys Ther 1996; 23: 200-208.
12. Wilson T, Kitsell F. Is the Q-angle an absolute or a variable measure? Physiotherapy 2002; 88: 296-302.
13. Merchant A, Fraiser A, Dragoo J, Fredericson M. A reliable Q angle measurement using a standardized protocol. Knee 2020; 73: 934-939.
14. Ando T, Hirose H, Inque M, Shino K, Doi T. A new method using computed tomographic scan to measure the rectus femoris-patellar tendon Q-angle comparison with conventional method. Clin Orthop 1993; 289: 213-219.
15. Biedert RM, Warnke K. Correlation between the Q angle and the patella position: A clinical and axial computed tomography evaluation. Arch Orthop Trauma Surg 2001; 121: 346-349.
16. Padash S, Mickley JP, Vera Garcia DV, Nugen F, Khosravi B, Erickson BJ, Wyles CC, Taunton MJ. An Overview of Machine Learning in Orthopedic Surgery: An Educational Paper. J Arthroplasty 2023; 38: 1938-1942.
17. Groot OQ, Bongers MER, Ogink PT, Senders JT, Karhade AV, Bramer JAM, Verlaan JJ, Schwab JH. Does artificial intelligence outperform natural intelligence in interpreting musculoskeletal radiological studies? A systematic review. Clin Orthop Relat Res 2020; 478: 2751-2764.
18. Rosset A, Spadola L, Ratib O. OsiriX: An Open-Source Software for Navigating in Multidimensional DICOM Images. J Digit Imaging 2004; 17: 205-216.
19. Pizer S, Amburn EP, Austin JD, Cromartie R, Geselowitz A, Greer T, Haar Romeny B, Zimmerman B, Zuiderveld K. Adaptive histogram equalization and its variations. Computer Vision, Graphics, and Image Processing 1987; 39: 355-368.
20. Lee H, Choo D, Le T, Bum J. Chest Radiographs Enhancement with Contrast Limited Adaptive Histogram. IMCOM Seoul, Republic of Korea 2023; 1-2.
21. Jocher G, Chaurasia A, Qiu J. YOLO by Ultralytics. 2023.
22. YOLO Object Detection Explained: Evolution, Algorithm, and Applications. 2024. Available at: https://encord.com/blog/yolo-object-detection-guide/

23. Morita D, Kawarazaki A, Soufi M, Otake Y, Sato Y, Numajiri T. Automatic detection of midfacial fractures in facial bone CT images using deep learning-based object detection models. J Stomatol Oral Maxillofac Surg 2024; 125: 101914.
24. Lin TY, Maire M, Belongie S, Bourdev L, Girshick R, Hays J, Perona P, Ramanan D, Zitnick CL, Dollár P. Microsoft COCO: Common Objects in Context. In: Fleet D, Pajdla T, Schiele B, Tuytelaars T. (eds) Computer Vision – ECCV 2014. Lecture Notes in Computer Science 2014; 8693: 740-755.
25. COCO – Common Objects in Context. Available at: https://cocodataset.org/#home
26. France L, Nester C. Effect of errors in the identification of anatomical landmarks on the accuracy of Q angle values. Clin Biomech 2001; 16: 710-713.
27. Chevidikunnana MF, Saif AA, Harish PK, Mathias L. Comparing goniometric and radiographic measurement of Q angle of the knee. Asian Biomed 2015; 9: 631-636.
28. Roush JR, Bustillo K, Low E. Measurement Error Between a Goniometer and the NIH ImageJ Program for Measuring Quadriceps Angle. Internet J Allied Health Sci Pract 2008; 6: 7.
29. Bhalara A, Talsaniya D, Ghandi N. Q Angle in Children Population Aged Between 7 To 12 Years. IJHSR 2013; 3: 57-64.
30. Veeramani R, Shankar N, Narayanan S, Ranganath P, Devi R. Bilateral Variability of the Quadriceps Angle (Q angle) in an Adult Indian Population. Iran J Basic Med Sci 2011; 14: 465-471.
31. Ayanniyi O, Alonge IA, Ogwumike O. Quadriceps Angle In Children With And Without Pes Planus. The Internet Journal of Health 2011; 12.
32. Markeas N, Kafalides G, Karakaidos D, Triantafyllides G, Efstathiadou H, Zossi P, Verdis A, Karis C. The values of Q angle in children (An epidemiology study). J Bone Joint Surg Br 2003; 85: S223-S224.